Analytical Methods

Assessment of quantitative accuracy of Rietveld/XRD analysis of the crystalline and amorphous phases in fly ash

Journal:	*Analytical Methods*
Manuscript ID	Draft
Article Type:	Paper
Date Submitted by the Author:	n/a
Complete List of Authors:	Zhao, Piqi; University of Jinan Liu, Xianping; Tongji University De la Torre, Angeles; University of Malaga, Lu, Lingchao; University of Jinan, School of materials science and engineering Sobolev, Konstantin; University of Wisconsin Milwaukee,

Journal Name

ARTICLE

Assessment of quantitative accuracy of Rietveld/XRD analysis of the crystalline and amorphous phases in fly ash

Received 00th January 20xx,
Accepted 00th January 20xx

DOI: 10.1039/x0xx00000x

www.rsc.org/

Piqi Zhao,[a†] Xianping Liu,[b] A.G. De La Torre[c], Lingchao Lu[a,†] and Konstantin Sobolev[d]

Abstract: The internal standard method based on Rietveld/XRD whole-patten fitting analysis of fly ash is used to assess the quantitative accuracy to determine the crystalline and amorphous phases under various conditions such as internal standards (types, SiO_2 or Al_2O_3 and dosages, 10-50%), incident X-rays (laboratory or synchrotron) and refinement software (GSAS or TOPAS). The results reveal that the quantitative stability is quite sensible to minor phases, identical to internal standard, in fly ash. Errors are positively correlated with the weight fraction of that minor phase, inclined to be ignored, and negatively correlated with the dosage of an internal standard and amorphous phase content in fly ash. The original formula for the amorphous phase calculation is not applicable for a case with a higher inherent SiO_2 content (>2.5%) in fly ash while the dosages of internal standard is lower than 20%. The original formula is modified as proposed. Based on it, the quantitative results of five different patterns report a good reproducibility with the arithmetic mean errors and the standard errors of identified main phases of around 1%.

1 Introduction

Fly ash (FA) has become one of the most attractive supplementary cementitious materials (SCM) since it was first developed to be high-volume fly ash concrete in the late 1980s [1]. It was reported that fly ash played a significant role in concrete performance, which show the acceptable early-age and long-term strength, low drying shrinkage and creep, and excellent durability when compared with Portland cement (PC) concrete with similar strength [2,3]. The morphology of fly ash particles (predominantly spherical in shape) provides considerable improvement of workability of fresh concrete [4]. The filler contribution and also pozzolanic effect are both beneficial to the long-term strength development and durability [5]. However, the mineralogical composition of fly ash, which depends on geological factors related to the formation and deposition of coal, its combustion condition and other factors, can be variable, leading to the fluctuations in performance and ineffective utilization [6]. In China, only about 40% of fly ash production is used in cement and concrete. One of the reasons for preventive effective utilization is related to lack of appropriate techniques for the characterization and screening of raw fly ash and identification of hydration products.

There are three methods commonly use to characterize the composition of fly ash: (1) X-ray fluorescence (XRF), (2) Energy-dispersive X-ray spectroscopy (EDS), and (3) X-ray diffraction (XRD). Widely accepted classification of fly ash is governed by Standards EN 197-1 [7], ASTM C618 [8] and GB 1596 [9]. However, the activity of fly ash cannot be estimated only based on the chemical composition from XRF analysis. Prior art demonstrated that fly ash had considerably different performance in concrete even though containing similar bulk chemical composition [10-13]. With EDS, according to the content of Al, Si and Ca, fly ash can be divided into several groups, possessing certain hydraulic activity [12, 14-15]. Combined with scanning electron microscope (SEM) or back scattered electron (BSE) images, EDS is an appropriate approach to study fly ash including the analysis of glass content and chemical composition of different products. The main obstacle of this method is that it requires large volumes of data to be analyzed and so this process is time-consuming. Unfortunately, EDS cannot distinguish the phases with similar elementary composition. XRD coupled with Rietveld refinement has been increasingly used as a fast and reliable method to evaluate the content of the crystalline and amorphous phases in inorganic materials [16]. The test is usually performed by spiking the crystalline samples of an internal standard such as SiO_2, Al_2O_3, or TiO_2 at a known proportion. This method has demonstrated a better adaptability in estimating the minor phases [17-18]. However, the Rietveld/XRD quantitative results can fluctuated depending on specimen preparation [19], radiation source [20]

[a] Shandong Provincial Key Laboratory of Preparation and Measurement of Building Materials, University of Jinan, Jinan 250022, China
[b] School of Materials Science and Engineering, Tongji University, Shanghai 201804, China
[c] Departamento de Química Inorgánica, Cristalografía y Mineralogía, Universidad de Málaga, Málaga 29071, Spain
[d] Department of Civil and Engineering, University of Wisconsin-Milwaukee, P.O. Box 784, Milwaukee, WI 53201, USA
† First author: mse_zhaopq@ujn.edu.cn
Corresponding author: mse_lulc@ujn.edu.cn

and the content and types of standard powder [16]. Indeed, the fly ash specimens are difficult to characterize by Rietveld/XRD method due to the presence of dominant amorphous phase and complicated crystal composition. Therefore, the quantitative phase analysis of fly ash by the Rietveld/XRD method needs further attention. In addition, the quantitative stability of this method must be clearly demonstrated

In this paper, the influence of internal standards (types and dosages), incident X-rays (laboratory or synchrotron) and refinement software (GSAS or TOPAS) on quantitative stability of Rietveld method is discussed. The sensitivity of the stability in respect of minor phase of SiO_2 in fly ash which is exactly identical to spiked standard is evaluated by the numerical simulation and error analysis. Additionally, the derivation of modified equation for calculation of amorphous phase is also reported. The main objective of reported work is to study the extent of quantitative stability of Rietveld method with various of the above comprehensive factors and propose modification for original formula of amorphous calculation.

2 Materials and Methods

2.1 Raw Materials

Fly ash supplied by Baotian New Type Building Material Co., Ltd (China) is quantitatively studied by Rietveld/XRD method. Chemical composition and particle size distribution data are reported in Table 1 and Figure 1, respectively. Standard powders of α-Al_2O_3 (code SRM-676a) and SiO_2 (code AB111366) are used in this work as the internal standard. Powder sample of α-Al_2O_3 and SiO_2 are produced and supplied by National Institute of Standards and Technology, NIST (USA) and ABCR GmbH. Co. KG (Germany), respectively. SiO_2 standard is sieved through 125 μm prior to be used.

Table 1 Chemical composition of fly ash determined by XRF.

Fig. 1. Particle size distribution of investigated specimens of fly ash. (black dots correspond to particle size distribution and squares provide the volume distribution)

2.2 Sample preparation

The SiO_2 powder (AB111366) used as an internal standard was separately mixed with fly ash by adding 50 wt%, 20 wt% and 10 wt%, (for specimens labeled as FA_$SiO_2$50%, FA_$SiO_2$20% and FA_$SiO_2$10%, respectively). The α-Al_2O_3 (SRM-676a) reference material was similarly mixed with the fly ash by adding 20 wt% (labeled as FA_$Al_2O_3$20%). The above mixtures were wet milled in planetary mill with anhydrous alcohol (20 wt%t) to narrow the grain size distribution and homogenize the blend. The resulting slurries were evaporated and subsequently finely dispersed by grinding in an agate mortar.

2.3 Data collection and processing

Chemical composition of investigated fly ash specimen was determined by XRF (SRS3400, Bruker AXS Corporation, Germany) and particle size distribution measurements were carried out by laser particle size analyzer (LS 230 from Beckman Coulter, USA). The laboratory X-ray powder diffraction patterns (LXRD) were recorded in Bragg-Brentano reflection geometry ($\vartheta/2\vartheta$) on an X'Pert MPD PRO diffractometer (PANalytical International Corporation, Netherland) and Rigaku X-ray diffractometer (D/max2550VB3+/PC from Rigaku International Corporation, Japan). The detailed instrument settings for LXRD are summarized in Table 2. The synchrotron X-ray diffraction (SXRD) experiments were performed at the beamline BL14B1 of Shanghai Synchrotron Radiation Facility in China. The experimental parameters for SXRD are listed in Table 3. All the above patterns were refined by the Rietveld method with GSAS-EXPGUI or TOPAS software.

Table 2 The instrument settings for LXRD

Table 3 Synchrotron XRD instrument settings

3 Results and Discussion

3.1 The variability of Rietveld quantitative analysis with different values of internal standard

Figure 2 shows LXRD pattern of fly ash collected in the PANalytical equipment. The identification of the crystalline phases gives mullite ($2SiO_2 \bullet 3Al_2O_3$) and quartz (SiO_2) as main phases, accompanied by some minor phases such as calcite ($CaCO_3$), magnetite (Fe_3O_4) and rutile (TiO_2). The background observed at the diffraction angle (2ϑ) ranged 16° to 36° was arched up, indicating a large amount of amorphous phase in fly ash. The direct Rietveld quantitaion of this spectrum would result in the overestimated quantitative results. The internal standard method based on the Rietveld refinement as a strategy can solve this problem by the adjustment of crystalline content based on an actual dosage of the standard, (Eq. 1) [16]. The weight percentage of crystalline phases can be calculated after acquiring the amorphous content (Eq. 2).

$$W_{\text{Amor}} = \frac{1-(W_S / W_S^{'})}{(1-W_S)} \quad (1)$$

$$W_{\alpha} = \frac{W_{\alpha}^{'}(1-W_{\text{Amor}}(1-W_S))}{1-W_S} \quad (2)$$

Where W_{Amor} is the weight fraction of amorphous or non-identified phases in sample; W_{α} (W_S) and $W_{\alpha}^{'}(W_S^{'})$ is the actual weight fraction and overestimated Rietveld quantitative result of the Phase α (internal standard), respectively.

Γ: TiO_2; Δ: $2SiO_2 \bullet 3Al_2O_3$; B: $CaCO_3$; N: $Ca(OH)_2$; Θ:SiO_2; Ω:CaO; M:Fe_3O_4

Fig. 2. LXRD pattern of fly ash collected in the PANalytical instrument

One of the requirements for the internal standard is that it should have a simple and known structure of high symmetry to avoid the excessive complexity of combined XRD pattern [21].

Moreover, it should present diffraction peaks non-overlapped with the sample, small particle size and liner absorption coefficient as similar as possible to that of the sample. The SiO_2 powder is selected as an internal standard due to the presence of characteristic-sharp diffraction peaks (non overlapped with those of the sample, high identification resolution and proximate mass absorption coefficient corresponding to the main phases of fly ash, which could decrease the quantitative errors in the process of refinement due to microabsorption effect [16]. However, it is also important to highlight that fly ash sample may also contains some quartz (Fig. 2). Normally, it is inclined to ignore the contribution of minor phase (<5%), assuming that the effects on accuracy can be negligible. To evaluate the effect on the refined weight fractions, the theoretical quantitative results and error analysis were performed. The results, corresponding to different dosages of SiO_2 (internal standard) and various presumptive weight fractions of SiO_2 (inherent phase in fly ash), were displayed in Fig 3. Here, Fig 3(a), (c) and (e) separately represent the theoretical calculation system in which the content of amorphous phase in fly ash are assumed to be 10 wt%, 20 wt% and 50 wt%. The conclusion can be drawn that the theoretical content of amorphous phase is positively correlated with given weight fraction of SiO_2 in fly ash and negatively correlated with the dosages of internal standard. The corresponding error analysis reported by Fig 3(b), (d) and (f)) reveals that the most serious error-zone appeared at the bottom right corner, which means the original equation for calculation of amorphous phase is not applicable for a case with a higher weight fraction of inherent SiO_2 in fly ash and lower dosages of internal standard. Based on the variation of assumed amorphous content from 10 wt% to 50 wt%, it is obvious that the quantitative errors dramatically decrease at a higher content of internal standard. The absolute and relative errors were larger than 5% and 10%, respectively, when the assumed amorphous content reach 50 wt% meanwhile the inherent SiO_2 content is larger than 2.5% and the dosages of internal standard is lower than 20%.

Fig. 3 Theoretical calculated results and error analysis for amorphous phase (the circles, squares and triangles correspond to theoretical quantitative results at the internal standard dosage of 10 wt%, 20 wt% and 50 wt%, respectively)

To eliminate the quantitative errors, the original Eq. (1) for calculation of amorphous phase was rescaled. Using Rietveld refinement, the modified equation for calculation of the amorphous in fly ash can be derived as following:

$$W_{S(FA+Sta)}' = \frac{m_{S(Sum)}}{m_{C(Sum)}} = \frac{m_{Sta} + m_{S(FA)}}{m_{Sta} + m_{C(FA)}} \quad (3)$$

$$m_{Sta} = W_S * m_{(Sum)} \quad (4)$$

$$m_{C(FA)} = m_{(Sum)}(1 - W_{Amor})(1 - W_S) \quad (5)$$

$$m_{S(FA)} = W_{S(FA)}' * m_{C(FA)} = W_{S(FA)}' m_{(Sum)}(1 - W_{Amor})(1 - W_S) \quad (6)$$

Using the equations above, the quantitative relationship between the content of amorphous phase and SiO_2 including both original SiO_2 in fly ash and SiO_2 from internal standard can be transformed to the Eq. (7), and the modified equation for calculation of the amorphous phase content can be proposed as Eq. (8).

$$\frac{W_{S(FA)}'(1 - W_{Amor})(1 - W_S) + W_S}{W_S + (1 - W_{Amor})(1 - W_S)} = W_{S(FA+Sta)}' \quad (7)$$

$$W_{Amor} = 1 - \frac{W_S(1 - W_{S(FA+Sta)}')}{(W_{S(FA+Sta)}' - W_{S(FA)}')(1 - W_S)} \quad (8)$$

where W_{Amor} is a weight fraction of amorphous or non-identified phases in fly ash; W_S represents weight fraction of added internal standard (SiO_2); $W_{S(FA+Sta)}'$ and $W_{S(FA)}'$ are Rietveld refined weight fractions of SiO_2 in fly ash with and without the internal standard, respectively.

The Rietveld quantitative phase analysis of LXRD pattern of FA (PANalytical) was implemented using the GSAS-EXPGUI software. To start the refinement project, crystal structure files (.cif), instrument function file (.prm) and initial peak shape parameters were firstly introduced into the algorithm. The starting structure models were adopted from literature: $2SiO_2 \bullet 3Al_2O_3$ [22], SiO_2 [23], $CaCO_3$ [24], Fe_3O_4 [25], CaO [22], $Ca(OH)_2$ [26] and TiO_2 [27] . The instrument function file was chosen based on $CuK\alpha_1$ as the incident X-ray and Germanium as the monochromator (monochromatic model with wavelength of 1.54056 and polarization fraction value of 0.8). In this work, pseudo-Voigt function [28] with asymmetry correction [29] was used and the related parameter GW, LY, S/L and H/L were initially set to 5 $(0.01º)^2$, 12 (0.01º), 0.02 and 0.02, respectively. The refined overall parameters were cell parameters, zero-shift error, peak shape parameters (GW and LY) and phase fractions. A lineal interpolation function was chosen to fit the background with polynomial term gradually increasing to 36. Peak shapes were fitted by refining the Gaussian contribution and Lorentzian contribution separately when appropriated. Each round of the Rietveld refinement, the modified parameters was evaluated by the variation of least-square R factor and the difference curve between the calculated and diffraction pattern. The least square calculation for Rietveld refinement was carried out several times under the condition of satisfactory fit until the parameter of final variable sum was less than 5. Figure 4 shows the Rietveld plots for the FA and Rietveld quantitative results are listed in Table 4 (where t '*wt* % Rietveld' stands for the direct Rietveld results, i.e. assuming 100 wt% of crystalline phases).

The Rietveld quantitative phase analysis of fly ash with different dosages of internal standard (50%, 20% and 10%) were successively performed by similar strategy. For example, the Rietveld plot obtained for FA_$SiO_2$50% at the final round of refinement is reported in Figure 5. A comparison (Figure 6) is made between the quantitative results obtained from original (Eq. (1)) and modified equation (Eq. (8)). The Rietveld

quantitative errors are distinct when the inherent minor phase is the same phase as internal standard. The Rietveld quantitative results of amorphous phase in FA_$SiO_2$50% by modified and original formula are 70.4 wt% and 75.3 wt%, respectively, with the absolute difference of 4.9%. For FA_$SiO_2$20% and FA_$SiO_2$10% specimens, the absolute differences are 7.8% (69.2 wt% vs. 77.0 wt%) and 8.7% (69.8 wt% vs.78.5 wt%), respectively. It is apparent that the quantitative differences between these two equations tended to be more significant at the reduced dosage of internal standard. The observed data have a good correspondence to the theoretical error analysis (Fig. 3). Compared with Rietveld quantitative analysis for the specimens at three dosages of the internal standard, reported in Figure 7, the maximum absolute differences of the phases are 1.2% (70.4%, 69.2% and 69.8%) for amorphous phase, 0.9% (21.8%, 22.4% and 22.7%) for mullite and 0.3% (5.1%, 5.2% and 5.4%) for quartz. This illustrates that the Rietveld quantitative results are quite stable at various dosages of SiO_2 used as internal standard from 10 wt% to 50 wt% when the modified equation is applied.

Γ: TiO_2; Δ: $2SiO_2 \bullet 3Al_2O_3$; B: $CaCO_3$; N: $Ca(OH)_2$; Θ:SiO_2; Ω:CaO; M:Fe_3O_4

Fig.4 Rietveld LXRD plots of fly ash (collected in PANalytical equipment), with GSAS-EXPGUI software.

Γ: TiO_2; Δ: $2SiO_2 \bullet 3Al_2O_3$; B: $CaCO_3$; N: $Ca(OH)_2$; Θ:SiO_2; Ω:CaO; M:Fe_3O_4

Fig.5 Rietveld LXRD plot of FA_$SiO_2$50% (collected in PANalytical equipment), with GSAS-EXPGUI software.

Fig.6 The amorphous content comparison between the quantitative results obtained from original and modified equation

Fig. 7 Rietveld quantitative stability of the main phases (a:Amorphous b:Mullite and c: quartz) in fly ash supported by the modified equation

3.2 The stability of Rietveld quantitative analysis with different X-ray sources

To evaluate the effect of the type of applied radiation on Rietveld quantitative stability, the XRD patterns of FA_$Al_2O_3$20% were recorded in typical laboratory conditions (labeled as FA_$Al_2O_3$20%(CuKα1,2)) and synchrotron radiation facility (FA_$Al_2O_3$20% (Synchrotron)). The α-Al_2O_3 (SRM-676a) was used as a different internal standard. The XRD patterns were processed using the TOPAS software instead of GSAS. For refinement procedure, the crystal structure files (.str) and X-ray pattern of FA_$Al_2O_3$20%(CuKα1,2) specimen were used. The diffraction peak with FP function at about 25° was subsequently inserted. The emission profile (.lam) was represented by CuKα5.lam and the slit parameters were selected according to the instrument settings listed in Table 2. In the initial refinement cycles the global parameters, i.e. zero error, air scattering factor, and phase scale factors, were refined. The background was fitted by Chebychev function with 5 or 6 terms of polynomial equation. Cell parameters, absorption factor and crystalline size and strain of the main crystal phases were carefully refined within constrained limits when necessary. The refinement was carried out by several cycles until the stable R factor and satisfactory fits were obtained. The final Rietveld plot is reported in Fig.8(a) and derived quantitative results including amorphous content (column '*wt* original sample, $CuK\alpha_{1,2}$) are provided in Table 4, being the amorphous content in fly ash 67.1 wt%, while the mullite and quartz phases are 23.3 wt% and 4.9 wt%, respectively. The FA_$Al_2O_3$20% (Synchrotron) specimen was continually refined by TOPAS software following similar strategy. The inserted amorphous phase peak was changed as the position of $2\vartheta \approx 20°$. The 'CuKα1.lam' file was used as the emission profile with the wavelength of 1.2379A. Polarization factor (LP) value was set to 90. The Rietveld plot and quantitative results are reported in Fig. 7 (b) and Table 4. The satisfactory refinement is achieved by achieving the adequate smoothness of the Yobs-Ycalc curve and low R factors (R_{WP}=7.8%, R_P=6.0%) confirming that the Rietveld quantitative analysis of fly ash sample was adequate. The Rietveld quantitative results provide the weight percentage of amorphous phase, mullite and quartz as 68.9 wt%, 23.9 wt% and 4.2 wt%, respectively.

Fig. 8 The Rietveld quantitative XRD pattern of FA_$Al_2O_3$20% sample : (a) FA_$Al_2O_3$20%(CuKα1,2), (b) FA_$Al_2O_3$20%(Synchrotron), with TOPAS software.

The Rietveld quantitative results with two different X-ray sources are compared and reported in the column of 'Absolute difference' (Table 4). It is demonstrated that the largest absolute differences (1.7%) are calculated for the amorphous phase fractions. Furthermore, results obtained using two refinements were plotted with respect to each other in Fig. 9. All values are located close to the 1:1 ratio bisector, which is also implying excellent reproducibility of the analyses. The error bars (esd), mostly smaller than the symbol size, are based on 3σ errors of phases as determined by the Rietveld refinement. Invariably, the esd values obtained from the laboratory experiments are larger relatively to the synchrotron esd values due to the reduced counting statistics. The reproducibility of the phase fraction calculations indicates that equivalent quantitative mineralogical analysis results of fly ash can be obtained from the laboratory equipment based on a careful analysis. The internal standard method based on the Rietveld refinement is a reliable analysis approach to quantify the crystalline and amorphous phases in fly ash.

Table 4 Rietveld quantitative phase analysis of FA_$Al_2O_3$20% sample using CuKα1,2 and Synchrotron

Fig. 9 The correlation plot of weight fractions refined from FA_$Al_2O_3$20%(CuKα1,2) and FA_$Al_2O_3$20%(Synchrotron).

3.3 The numerical analysis for Rietveld quantitative results

The consistency of Rietveld quantitative analysis is the main prerequisite to ensure its correct application. Though internal standard method based on Rietveld refinement can be used for quantitative phase analysis of materials with both crystalline and amorphous phases, the use of internal standard makes the quantitation of phases in fly ash specimens more complicated. Such complication can lead to the fluctuation of quantitative results at different external conditions such as types and dosages of internal standards, incident X-rays and refinement softwares. The Rietveld quantitative stability is further compared for fly ash patterns FA_$SiO_2$50% (CuKα1_GSAS), FA_$SiO_2$20% (CuKα1_GSAS), FA_$SiO_2$10% (CuKα1_GSAS), FA_$Al_2O_3$20% （CuKα1,2_TOPAS）and FA_$Al_2O_3$20%(Synchrotron_TOPAS). The weight percentage of mullite, quartz and amorphous phase in fly ash is respectively calculated by arithmetic mean to be 22.8 wt%, 4.9 wt% and 69.1 wt%, introduced as horizontal line in the Fig. 10. The arithmetic mean error δ and standard error s are calculated to evaluate the quantitative stability, where errors are listed as δ(mullite)=0.6%, δ(quartz)=0.3%, δ(amorphous)=0.9%, s(mullite)=±0.8%, s(quartz)=±0.5% and s(amorphous)=±1.2%, respectively. It is apparent that the arithmetic mean errors and the standard errors of the main phases were all around 1%, indicating that the results had less fluctuation at high stability of the quantitative phase analysis. Good reproducibility of phase fraction quantitation indicates that the equivalent quantitative results can be obtained by Rietvled refinement method based on using internal standard. The results are only little influenced by the external factors such as the type and dosage of internal standard, incident X-ray and refinement software if a careful analysis is carried out.

4 Conclusions

The ignorance of a minor phase in sample which is identical to the internal standard, has significant effect on the Rietvled quantitative phase analysis to derived amorphous contents. Theoretical errors are positive correlated with the weight fraction of ignored phase and negatively correlated with the dosages of internal standard and actual weight fraction of amorphous component in sample. The original equation for amorphous phase calculation is not applicable for a case with a higher inherent SiO_2 content (>2.5%) in fly ash while the dosages of internal standard is lower than 20%.

The modified equation for amorphous calculation based on the internal standard is suggested. The absolute difference in the amorphous content in fly ash between the modified and original formula is 4.9% in FA_$SiO_2$50% (50 wt% of internal standard), 7.8% in FA_$SiO_2$20% (20 wt% of internal standard) and 8.7% in FA_$SiO_2$10% (10 wt% of internal standard) The Rietveld quantitative results are quite stable at various dosages of SiO_2 as internal standard from 10 wt% to 50 wt% under the precondition of modified formula application. The maximum absolute differences of the same phases include the amorphous and main crystalline phases such as mullite and quartz are respectively 1.2%, 0.9% and 0.3%.

The quantitative analysis of fly ash obtained by Rietvled/XRD method based on the addition of internal standard has a good reproducibility, stable to the fluctuation of external factors such as spiked standards (types and dosages), incident X-rays and refinement softwares. The arithmetic mean errors and the standard errors of the main phases were all around 1%.

Fig. 10 Comparison of the Rietveld quantitative results of the same fly ash sample. Horizontal lines are the arithmetic mean values.

Acknowledgements

The access to the beamline BL14B1 facilities at the SSRF is appreciated and the support of SSRF management, User Office and beamline staff is highly appreciated. This Research is supported by the National Natural Science Foundation of China (No.51602126 and 51102181) and the Program for Scientific Research Innovation Team in Colleges and Universities of Shandong Province.

Notes and references

1 Malhotra VM, Superplasticized fly ash concrete for structural applications, *Concr Int*, 1986, **8**: 28-31.
2 Carette G, Mechanical properties of concrete incorporating high volumes of fly ash from sources in the U.S, *ACI Materials Journal*, 1993, **90**.
3 Mcdonald D, Durability of concrete incorporating high volumes of fly ash from sources in the U.S, *ACI Materials Journal*, 1994, **91**: 632-633.
4 Wang A, Zhang C, Sun W (2003) Fly ash effects: I. The morphological effect of fly ash, *Cement and Concrete Research* **33**:2023-2029.
5 Wang A, Zhang C, Sun, W, Fly ash effects: II the active effect of fly ash. *Cement & Concrete Research*, 2004, **34**:2057-2060.
6 Ahmaruzzaman M, A review on the utilization of fly ash, *Progress in Energy & Combustion Science*, 2010, **36**:327-363.
7 E. 197-1, Cement. Part 1: Composition, specifications and conformity criteria for common cements, 2011.
8 A.S.f. Testing, Materials, Standard specification for coal fly ash and raw or calcined natural pozzolan for use in concrete, *ASTM International*,2008.
9 GB/T 1596 Fly ash used in cement or concrete, 2005.
10 Schlorholtz S, Demirel K B T, Monitoring of fluctuations in the physical and chemical properties of a high-calcium fly ash.*Mrs Online Proceeding Library*, 1986, **113**.
11 Mehta P K, Pozzolanic and Cementitious by-Products in Concrete--Another Look, *Special Publication,* 1989, **114**:1-44.
12 Durdziński PT, Dunant CF, Haha MB et al, A new quantification method based on sem-eds to assess fly ash composition and study the reaction of its individual components in hydrating cement paste, *Cement & Concrete Research*, 2015, **73**:111-122.
13 Chancey RT, Stutzman P, Juenger MCG et al, Comprehensive phase characterization of crystalline and amorphous phases of a class F fly ash, *Cement & Concrete Research,* 2010, **40**:146-156.
14 Nathan Y, Dvorachek M, Pelly I et al, Characterization of coal fly ash from israel, *Fuel* ,1999, **78**: 205-213.

15 Kutchko BG, Kim AG, Fly ash characterization by sem–eds, *Fuel* 2006, **85**:2537-2544.
16 De la Torre AG, Bruque S, Aranda MAG, Rietveld quantitative amorphous content analysis, *Journal of Applied Crystallography* , 2001, **34**:196-202.
17 Winburn RS, Grier DG, Rietveld quantitative X-ray diffraction analysis of nist fly ash standard reference materials, *Powder Diffraction,* 2000, **15**:163-172.
18 Winburn RS, Lerach SL, Mccarthy GJ et al, Quantification of ferrite spinel and hematite in fly ash magnetically enriched fractions, *Advances in X-ray Analysis*, 2000, **43**:350-355.
19 Aranda MAG, De la Torre AG, Leon-Reina L, Rietveld quantitative phase analysis of opc clinkers, cements and hydration products, *Reviews in Mineralogy & Geochemistry,* 2012,**74**:169-209.
20 De la Torre AG, Aranda MAG, Accuracy in rietveld quantitative phase analysis of portland cements, *Journal of Applied Crystallography*, 2003, **36**:1169-1176.
21 Post JE, Bish DL, Rietveld refinement of crystal structures using powder X-ray diffraction data, *Reviews in Mineralogy,* 1989, **20**:277-308.
22 Sadanaga R, Tokonami M, Takeuchi Y et al, The structure of mullite, $2Al_2O_3$. SiO_2, and relationship with the structures of sillimanite andandalusite. *Acta Crystallographica,* 1962, **15**: 65-68.
23 Will G, Bellotto M, Parrish W et al. Crystal structures of quartz and magnesium germanate by profile analysis of synchrotron-radiation high-resolution powder data. *Journal of Applied Crystallography* , 1988, **21**:182-191.
24 Maslen EN, Streltsov VA, Streltsova NR et al. Electron density and optical anisotropy in rhombohedral carbonates. iii. synchrotron X-ray studies of $CaCO_3$, $MgCO_3$ and $MnCO_3$, *Acta Crystallographica Section B,* 1995, **51**:929-939.
25 Fleet ME, The structure of magnetite: two annealed natural magnetites, $Fe_{3.005}O_4$, and $Fe_{2.96}Mg_{0.04}O_4$, Acta Crystallographica Section C: *Crystal Structure Communications* , 1984, **40**: 1491-1493.
26 Petch HE, The hydrogen positions in portlandite, Ca $(OH)_2$, as indicated by the electron distribution, *Acta Crystallographica,* 1961, **14**:950-957.
27 Baur WH, Khan AA, Rutile-type compounds. IV. SiO_2, GeO_2 and a comparison with other rutile-type structures, *Acta Crystallographica Section B* ,1971, **27**:2133-2139.
28 Thompson P, Cox DE, Hastings JB, Rietveld refinement of debye–scherrer synchrotron x-ray data from Al_2O_3, *Journal of Applied Crystallography , 1987,* **20**:79-83.
29 Finger LW, Cox DE, Jephcoat AP, A correction for powder diffraction peak asymmetry due to axial divergence, *Journal of Applied Crystallography, 1994,* **27**:892-900.

Statement of Societal Impact

Fly ash, the most attractive supplementary cementitious materials, plays a significant role in concrete performance. However, the quality of fly ash is irregularity, leading to the fluctuations in performance even damage to buildings. So it is necessary to evaluate the quality including quantitative phase analysis before using it. Although XRD coupled with Rietveld refinement has been demonstrated as an effective analysis method, some factors that inclined to be ignored in fly ash system still need further consideration to guarantee the quantitative accuracy and stability. In this work, assessment of quantitative accuracy of Rietveld/XRD analysis of the crystalline and amorphous phases in fly ash was systematically investigated. The main contribution of this work can be summarized as follows,

Firstly, this study has identified minor phase in sample which is identical to the internal standard has significant effect on the Rietvled quantitative phase analysis to derived amorphous contents, however, the contribution was ignored before. Errors deviation and correlation analysis were further performed. Secondly, based on the error analysis, the corrected equation for Rietveld quantitative phase analysis of amorphous was submitted. The quantitative analysis of fly ash obtained by Rietvled/XRD method based on the corrected equantion has a much

better reproducibility, more accurate and stable toward the fluctuation of external factors such as spiked standards (types and dosages), incident X-rays and refinementsoftwares.

I think it is a new topic and challenge.

Thank you for your consideration and best regards.

Yours sincerely,

Lingchao LU

University of Jinan

Jinan, China

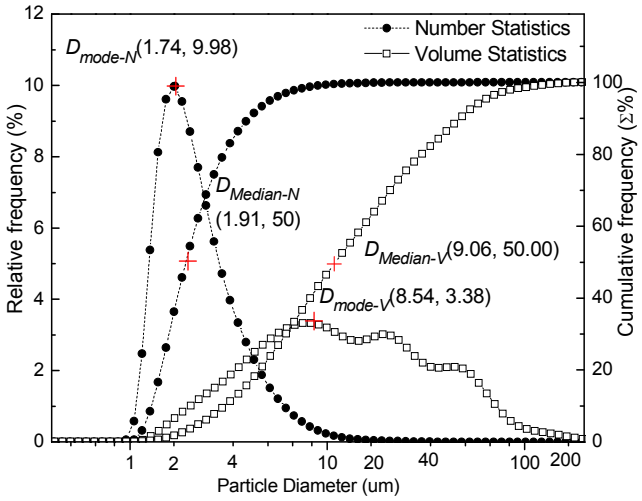

Fig. 1. Particle size distribution of investigated specimens of fly ash. (black dots correspond to particle size distribution and squares provide the volume distribution)

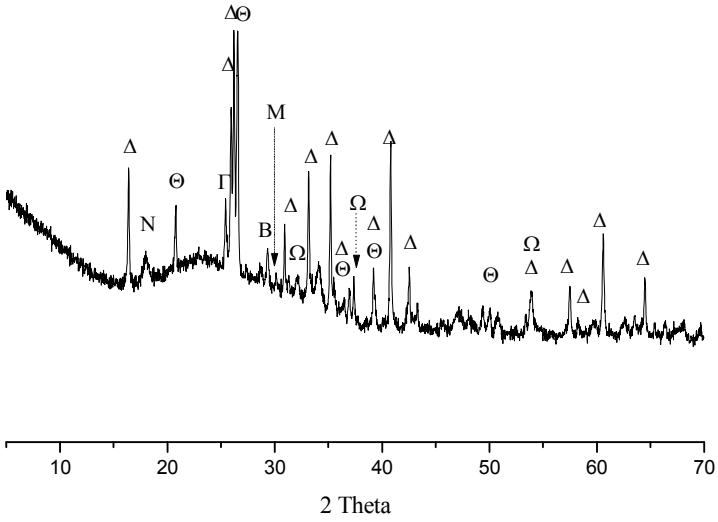

Γ: TiO_2; Δ: $2SiO_2 \cdot 3Al_2O_3$; B: $CaCO_3$; N: $Ca(OH)_2$; Θ:SiO_2; Ω:CaO; M:Fe_3O_4

Fig. 2. LXRD pattern of fly ash collected in the PANalytical instrument

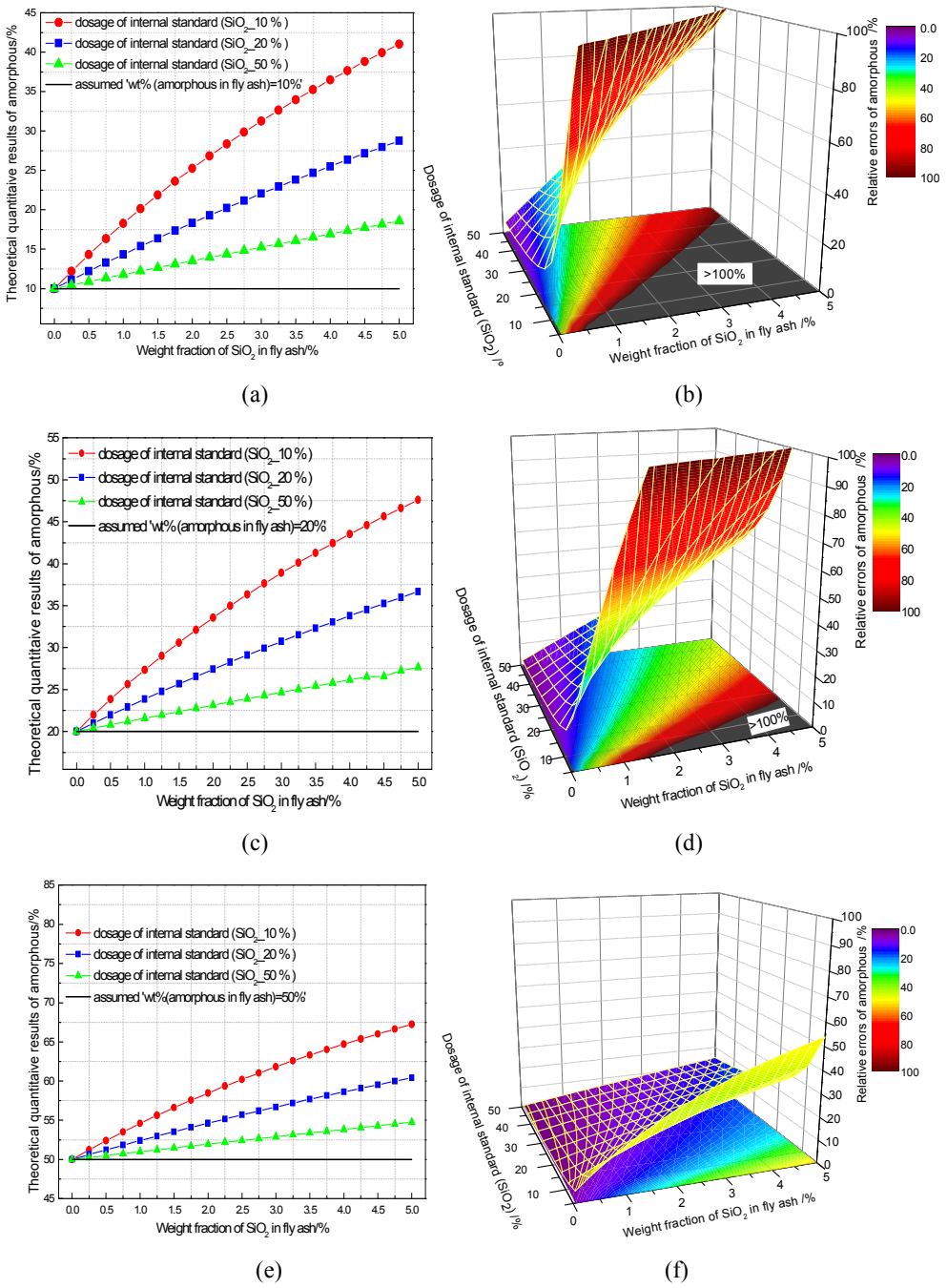

Fig. 3 Theoretical calculated results and error analysis for amorphous phase (the circles, squares and triangles correspond to theoretical quantitative results at the internal standard dosage of 10 wt%, 20 wt% and 50 wt%, respectively)

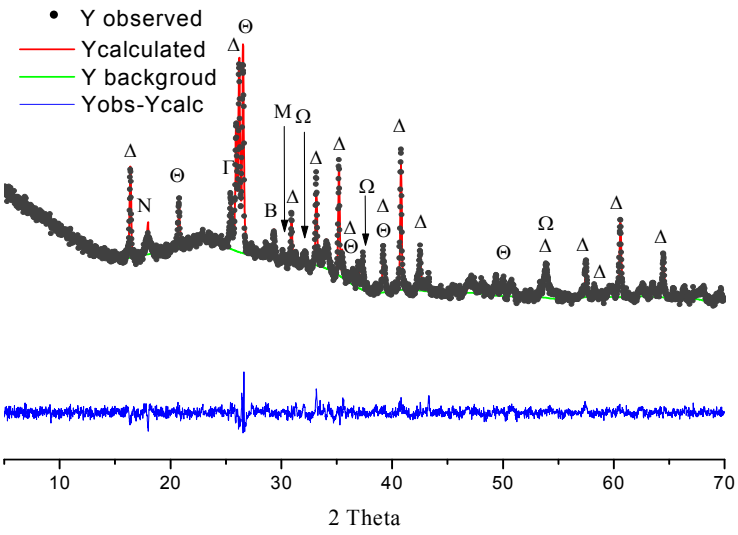

Γ: TiO_2; Δ: $2SiO_2•3Al_2O_3$; B: $CaCO_3$; N: $Ca(OH)_2$; Θ:SiO_2; Ω:CaO; M:Fe_3O_4

Fig.4 Rietveld LXRD plots of fly ash (collected in PANalytical equipment), with GSAS-EXPGUI software.

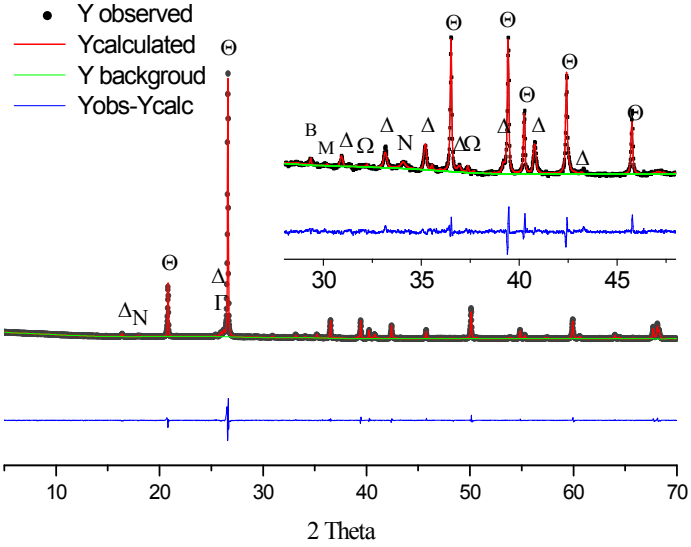

Γ: TiO_2; Δ: $2SiO_2•3Al_2O_3$; B: $CaCO_3$; N: $Ca(OH)_2$; Θ:SiO_2; Ω:CaO; M:Fe_3O_4

Fig. 5 Rietveld LXRD plot of FA_$SiO_2$50% (collected in PANalytical equipment), with GSAS-EXPGUI software.

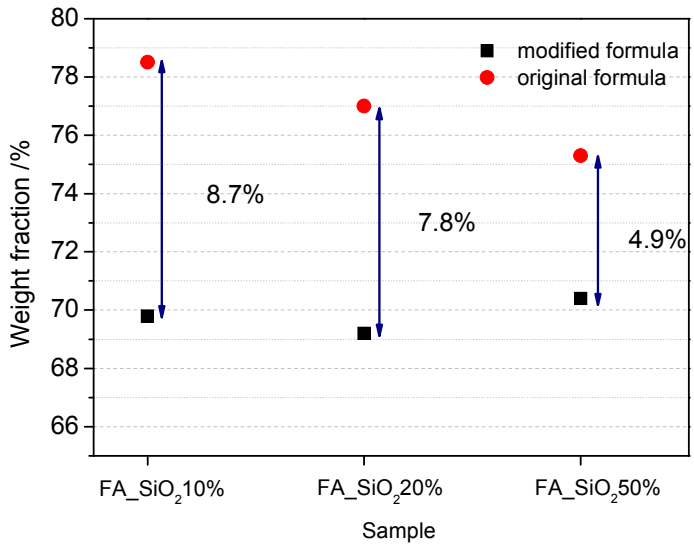

Fig. 6 The amorphous content comparison between the quantitative results obtained from original and modified equation

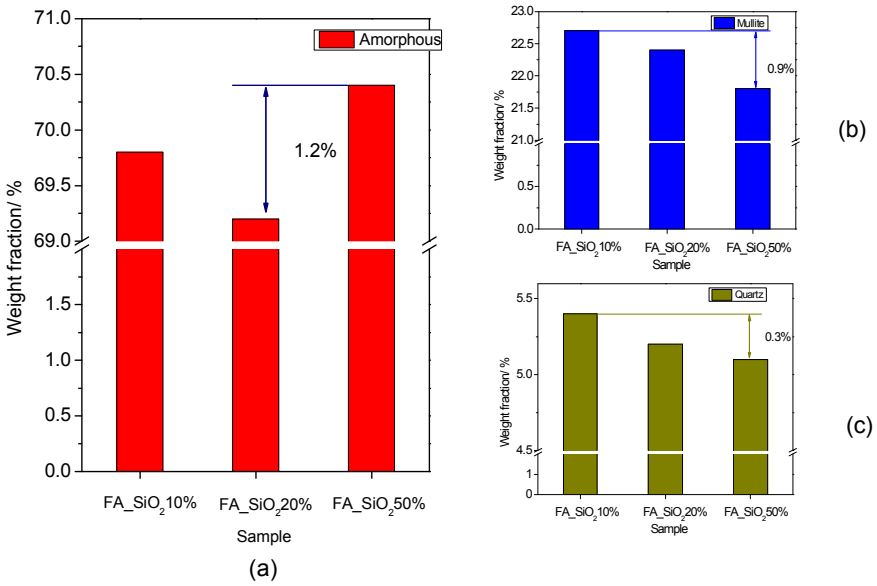

Fig. 7 Rietveld quantitative stability of the main phases (a:Amorphous b:Mullite and c: quartz) in fly ash supported by the modified equation

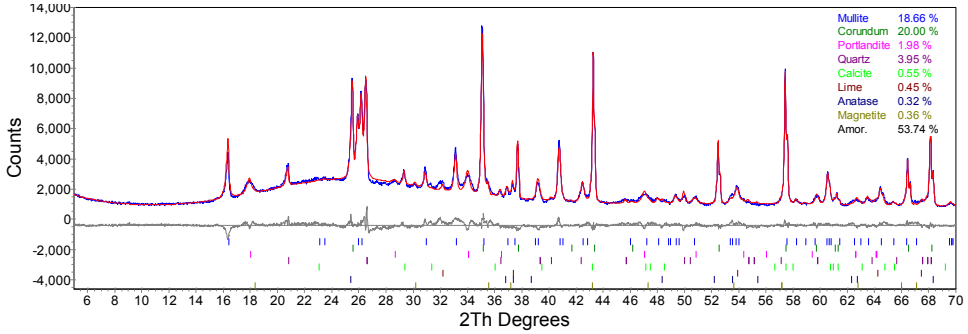

(a)

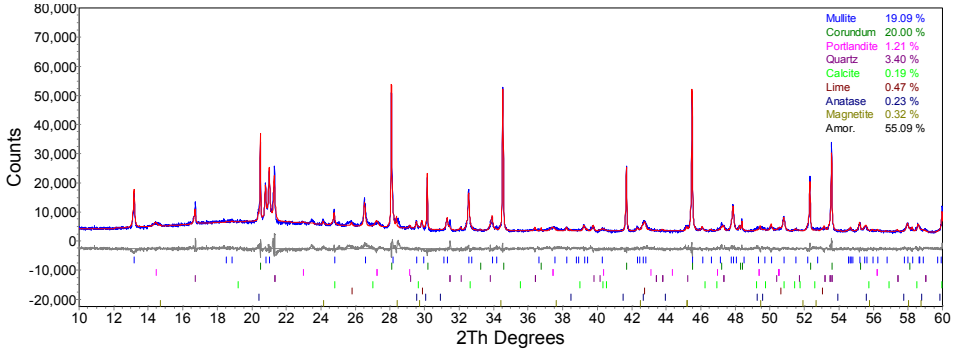

(b)

Fig. 8 The Rietveld quantitative XRD pattern of FA_$Al_2O_3$20% sample : (a) FA_$Al_2O_3$20%(CuKα1,2), (b) FA_$Al_2O_3$20%(Synchrotron), with TOPAS software.

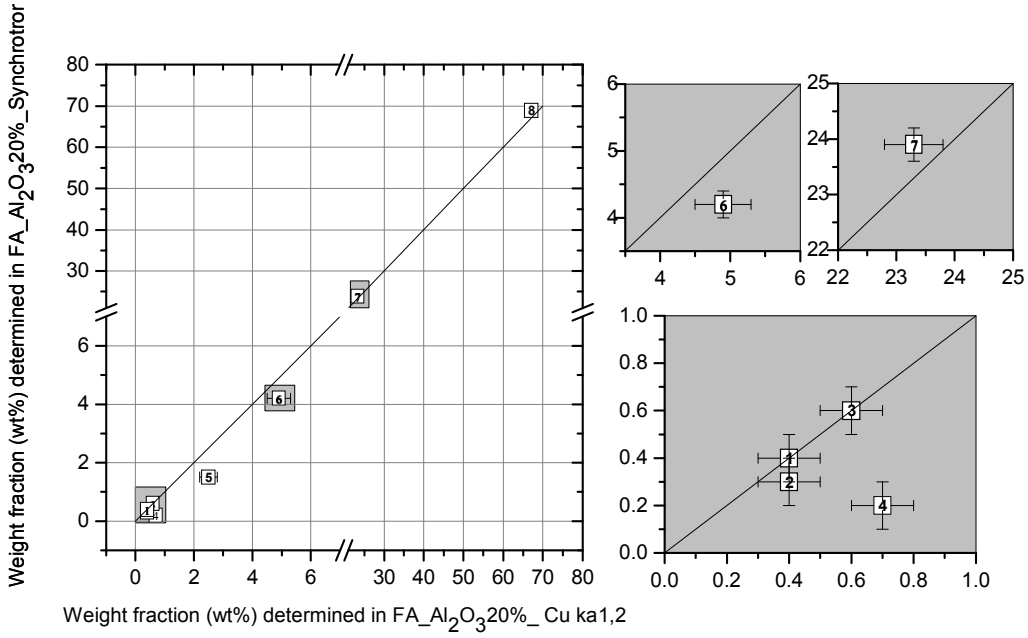

1: Fe_3O_4 **2:** TiO_2 **3:** CaO **4:** $CaCO_3$ **5:** $Ca(OH)_2$ **6:** SiO_2 **7:** $2SiO_2•3Al_2O_3$ **8:** Amorphous

Fig. 9 The correlation plot of weight fractions refined from FA_$Al_2O_3$20%(CuKα1,2) and FA_$Al_2O_3$20%(Synchrotron).

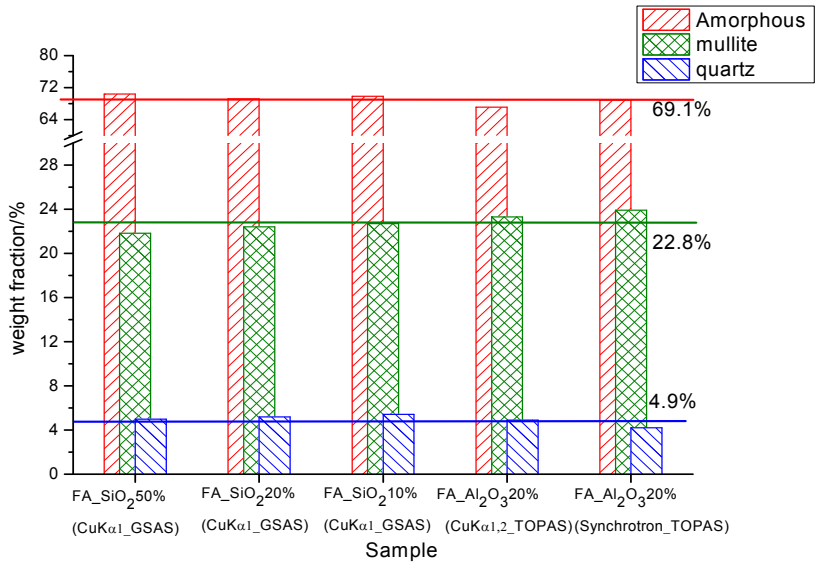

Fig. 10 Comparison of the Rietveld quantitative results of the same fly ash sample. Horizontal lines are the arithmetic mean values.

Table 1 Chemical composition of fly ash determined by XRF.

Oxide Composition	Na_2O	MgO	Al_2O_3	SiO_2	SO_3	K_2O	CaO	TiO_2	Fe_2O_3	LoI*
Content (wt%)	0.64	0.77	25.6	44.9	0.60	1.01	7.99	0.96	4.98	3.57

* Loss on Ignition

Table 2 The instrument settings for LXRD

Parameters \ Manufacturers	PANalytical	Rigaku
Scanning type	Continuous scanning	Step scanning
X-ray radiation	$CuK\alpha_1$, 45 kV/40 mA	$CuK\alpha_{1,2}$, 40kV/250mA
Detector	X´Celerator detector	Point detctor
Monochromator	Ge (111)	C (002)
Divergence slit /°	1/2	1/2
Anti-scatter slit /°	1/2	1/2
Receiving slit /mm	–	0.15
Soller slit(rad)	0.04	–
Angular range, 2θ /°	5–70	5–70
Step width /°	0.0167	0.02
Measure time /h	2	4.5
Sample spinning speed (r.p.m)	15	15
Geometry	Reflection/flat sample	Reflection/flat sample

Table 3 Synchrotron XRD instrument settings

Content	SXRD
Scanning type	Step scanning
Wavelength/ Å	1.2379
Monochromator (Crystal type)	Si(111)
Angular range, 2θ /°	10–60
Step width /°	0.01
Count time per step /s	0.5
Geometry	Reflection/flat sample

Table 4 Rietveld quantitative phase analysis of FA_$Al_2O_3$20% sample using CuKα1,2 and Synchrotron

Analysis	Phases and *R*-factors	*wt* % in original sample (CuKα1,2)	*Wt%* in original sample (Synchrotron)	Absolute difference
Quantitative results	$2SiO_2•3Al_2O_3$	23.3(4)	23.9(2)	0.6
	Al_2O_3	—	—	—
	$Ca(OH)_2$	2.5(3)	1.5(1)	1.0
	SiO_2	4.9(4)	4.2(2)	0.7
	$CaCO_3$	0.7(1)	0.2(1)	0.5
	CaO	0.6(1)	0.6(1)	0
	TiO_2	0.4(1)	0.3(1)	0.1
	Fe_3O_4	0.4(1)	0.4(1)	0
	Amorphous	67.2	68.9	1.7
Criteria of fit	R_{WP}	6.3	7.8	—
	R_P	4.8	6.0	—

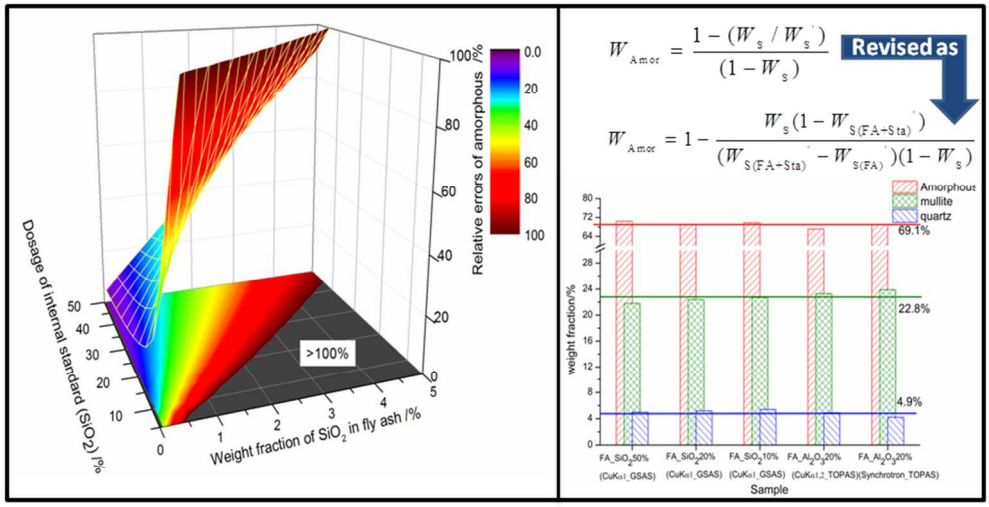

The revised equation for amorphous based on the internal standard is proposed

254x142mm (96 x 96 DPI)